Large-Scale Regioselective Formation of Well-Defined Stable Wrinkles of Multilayered Films via Embossing

Conghua Lu,*[,†,‡] Helmuth Möhwald,[†] and Andreas Fery*[,§]

Interface Department, Max Planck Institute of Colloids and Interfaces, Potsdam 14424, Germany, and Department of Physical Chemistry, University of Bayreuth, Bayreuth 95440, Germany

Received July 9, 2008. Revised Manuscript Received September 24, 2008

We report on large-scale fabrication of wrinkled polyelectrolyte multilayers (PEMs) with well-defined surface relief structures by *embossing*. The embossed assembly films show hierarchical topography consisting of patterns on the micrometer scale defined by the stamp used for embossing that are decorated by stable and highly regular patterns on the submicrometer scale. The periodicities of the concentric wrinkles can be controlled well down to 250 nm. We propose that a new mechanism of combining inelastic deformation of the support and selective wetting by the PEM film to be responsible for the above wrinkling with high stability in the wet state and enhanced aspect ratio.

Introduction

Micro/nanostructured surfaces have a wide range of prospective applications in fundamental research, and applications in nanotechnology require mastering the structuring process.[1] So far lithographic techniques are mainly used to fabricate structured surfaces, and the fabrication of sub-100 nm features using lithography has well been established. Considering the complicated process and high demand for the rigorous operation conditions, there is a strong need for alternative simple and versatile approaches for structuring in this regime.

Recently, controlled buckling or wrinkling has attracted intensive interest as an alternative pathway toward structuring on the micrometer- and submicrometer scale.[2−7] In buckling or wrinkling, shape changes take place as a result of mechanical instability,[2−11] while this phenomenon is often rather difficult to control due to its highly nonlinear nature. Recently, several situations have been identified in which sinusoidal wrinkles with controlled periodicity (or wavelength, λ) and amplitude can be produced. One such situation is mechanical deformation of elastomeric (soft) substrates covered by thin, hard layers.[2−11] In this case, wrinkle wavelengths spanning from several nanometers to many micrometers can be predicted even by analytical theories[12,13] and fine-tuned by choice of elastic constants of substrate/film and film thickness, respectively.[8,14−18] The typical substrate is a poly(dimethylsiloxane) (PDMS) elastomeric sheet, while the top thin hard layer of various materials can be designed according to the demands and fabricated by spin-coating,[8,17] layer-by-layer (LbL) self-assembly,[14−16,18] or vacuum deposition.[2,4] Among those, LbL self-assembly is a very simple and versatile method to build ultrathin composite multilayers with well-defined nanostructures including the composition, the thickness, the surface functional groups, and the internal linkage of layers.[19] For instance, the linear dependency of the wrinkle's wavelength on the thickness of the LbL assembly films has been checked experimentally.[14,15] The latter can be controlled at the

* To whom correspondence should be addressed. E-mail: luconghua@pku.org.cn (C.L.), andreas.fery@uni-bayreuth.de (A.F.). Tel: 0049-(0)331-5679171. Fax: 0049-(0)331-5679202.

† Max Planck Institute of Colloids and Interfaces.

‡ Current address: School of Materials Science and Engineering, Tianjin University, Tianjin 300072, P.R. China.

§ University of Bayreuth.

(1) (a) Xia, Y. N.; Rogers, J. A.; Paul, K. E.; Whitesides, G. M. *Chem. Rev.* **1999**, *99*, 1823. (b) Gates, B. D.; Xu, Q. B.; Stewart, M.; Ryan, D.; Willson, C. G.; Whitesides, G. M. *Chem. Rev.* **2005**, *105*, 1171.
(2) Bowden, N.; Brittain, S.; Evans, A. G.; Hutchinson, J. W.; Whitesides, G. M. *Nature* **1998**, *393*, 146.
(3) Sharp, J. S.; Jones, R. A. L. *Adv. Mater.* **2002**, *14*, 799.
(4) Yoo, P. J.; Suh, K. Y.; Park, S. Y.; Lee, H. H. *Adv. Mater.* **2002**, *14*, 1383.
(5) Efimenko, K.; Rackaitis, M.; Manias, E.; Vaziri, A.; Mahadevan, L.; Genzer, J. *Nat. Mater.* **2005**, *4*, 293.
(6) Genzer, J.; Groenewold, J. *Soft Matter* **2006**, *2*, 310.
(7) Moon, M.-W.; Lee, S. H.; Sun, J.-Y.; Oh, K. H.; Vaziri, A.; Hutchinson, J. W. *Proc. Natl. Acad. Sci. U.S.A.* **2007**, *104*, 1130.
(8) Stafford, C. M.; Harrison, C.; Beers, K. L.; Karim, A.; Amis, E. J.; Vanlandingham, M. R.; Kim, H. C.; Volksen, W.; Miller, R. D.; Simonyi, E. E. *Nat. Mater.* **2004**, *3*, 545.
(9) Okayasu, T.; Zhang, H. L.; Bucknall, D. G.; Briggs, G. A. D. *Adv. Funct. Mater.* **2004**, *14*, 1081.
(10) Huang, J. S.; Juszkiewicz, M.; de Jeu, W. H.; Cerda, E.; Emrick, T.; Menon, N.; Russell, T. P. *Science* **2007**, *317*, 650.
(11) Lin, P. C.; Yang, S. *Appl. Phys. Lett.* **2007**, *90*, 241903.
(12) Huang, Z. Y.; Hong, W.; Suo, Z. *J. Mech. Phys. Solids* **2005**, *53*, 2101.
(13) Jiang, H. Q.; Khang, D.-Y.; Song, J. Z.; Sun, Y. G.; Huang, Y. G.; Rogers, J. A. *Proc. Natl. Acad. Sci. U.S.A.* **2007**, *104*, 15607.
(14) (a) Nolte, A. J.; Rubner, M. F.; Cohen, R. E. *Macromolecules* **2005**, *38*, 5367. (b) Nolte, A. J.; Cohen, R. E.; Rubner, M. F. *Macromolecules* **2006**, *39*, 4841.
(15) (a) Lu, C. H.; Dönch, I.; Nolte, M.; Fery, A. *Chem. Mater.* **2006**, *18*, 6204. (b) Lu, C. H.; Möhwald, H.; Fery, A. *Soft Matter* **2007**, *3*, 1530.
(16) (a) Jiang, C. Y.; Singamaneni, S.; Merrick, E.; Tsukruk, V. V. *Nano Lett.* **2006**, *6*, 2254. (b) Gunawidjaja, R.; Ko, H.; Jiang, C.; Tsukruk, V. V. *Chem. Mater.* **2007**, *19*, 2007.
(17) Qian, W.; Xing, R.; Yu, X. H.; Quan, X. J.; Han, Y. C. *J. Chem. Phys.* **2007**, *126*, 064901.
(18) Hendricks, T. R.; Lee, I. *Nano Lett.* **2007**, *7*, 372.
(19) (a) Decher, G. *Science* **1997**, *277*, 1232. (b) Caruso, F.; Caruso, R. A.; Möhwald, H. *Science* **1998**, *282*, 1111. (c) Decher, G.; Schlenoff, J. B. *Multilayer Thin Films*; Wiley-VCH: Weinheim, Germany, 2003. (d) Ariga, K.; Hill, J. P.; Ji, Q. M. *Phys. Chem. Chem. Phys.* **2007**, *9*, 2319. (e) De Geest, B. G.; Sanders, N. N.; Sukhorukov, G. B.; Demeester, J.; De Smedt, S. C. *Chem. Soc. Rev.* **2007**, *36*, 636. (f) Quinn, J. F.; Johnston, A. P. R.; Such, G. K.; Zelikin, A. N.; Caruso, F. *Chem. Soc. Rev.* **2007**, *36*, 707.

10.1021/cm8018742 CCC: $40.75
Published on Web 10/29/2008

molecular scale via the deposition times and conditions for these systems.[19] So far, inorganic films and polymer-based composite films including nanoparticles,[15a,16a,18] one-dimensional nanowires,[16b] nanoribbons,[20a] and nanotubes[20b] have been fabricated to control the formation of wrinkles. Recently, a combination of buckling instability and micropattern templates has been utilized to further realize the regioselective formation of wrinkles with improved regularity and orientation. One way is to form a patterned film on a PDMS substrate followed by heating[2,21,22] or by uniaxial stretch (or compression) or on a prestrained PDMS support followed by releasing the strain.[20] The other is to *conformally contact* a film-coated PDMS compliant foundation with a soft structured template followed by heating[4] or solvent treatment.[17] Although much progress has been made in the control over the surface wrinkles, realization of stable and ordered surface wrinkles with controllable geometries and spatial locations is still a challenging task.

In this manuscript, we report on large-scale fabrication of wrinkled polyelectrolyte multilayers (PEMs) with well-defined surface relief structures by *embossing*. The embossed assembly films have novel concentric defect-free wrinkles, which have not been reported so far. Furthermore, the periodicities of the wrinkles of PEMs can be controlled well down to 250 nm. They are substantially stable even in the wet state, in drastic contrast with the previously reported wrinkles of polyelectrolyte multilayers, which are unstable in the case of exposure to water.[14a,15b,23] This is most important as most of the use of patterned surfaces involved adsorption from fluid phase. This high stability is achieved via a new mechanism where a supporting layer is inelastically and hence permanently deformed. This leads to a contrast in wettability as will be explained later. It also enables us to achieve high aspect ratios of patterns. We expect that the as-prepared wrinkles have promising applications as optical gratings,[24] electronic devices[20] and structured substrates directing the deposition and assembly of cells and other particles[15b,25] and in controlling wettability[26] and surface adhesion.[21]

Experimental Section

Materials. Poly(sodium 4-styrene sulfonate) (PSS, molecular weight ~ 100 000), poly(diallyldimethyl ammonium chloride) (PDDAC, 20 wt % molecular weight ~ 100 000−200 000), and poly(ethylenimine) (PEI, molecular weight ~25 000) were purchased from Sigma-Aldrich, and 1*H*,1*H*,2*H*,2*H*-perfluorodecylmethyldichlorosilane was from Alfa. All chemicals were used without any purification. One milligram per milliliter of the above single component of polyelectrolyte aqueous solution containing 0.15 M NaCl was prepared in Milli-Q water.

A poly(dimethylsiloxane) (PDMS) sheet with a thickness of ~1 mm was prepared by mixing the curing agent and base monomer (Sylgard 184, Dow Corning) at a 1:10 ratio (by weight) and casting into a tray. After degassing for 30 min, the mixture was baked at 60 °C for 12 h. To obtain a hydrophilic surface, the PDMS sheet was treated with air plasma (Harrick PDC 32G) at a pressure of 0.02 mbar with low intensity for 2 min and then immersed in 1 mg/mL PEI solution for later film assembly. The structured silicon master with the height of the protruding part of 10 μm was cleaned with piranha solution (H_2SO_4/H_2O_2; 7:3 (v/v), CAUTION: *piranha solution reacts violently with organic materials, handle with extreme caution*) for 10 min followed by thorough water washing. The cleaned master was modified with 1% (v/v) 1*H*,1*H*,2*H*,2*H*-perfluorodecylmethyldichlorosilane in 2,2,4-trimethylpentane solution for 5 min to form a perfluorinated layer on its surface.[27] After washing with *n*-hexane and chloroform, the substrate was air-dried for the subsequent processing.

Fabrication of PDDAC/PSS Multilayer Films on a PDMS Sheet. Spraying the assembly of $(PDDAC/PSS)_n$ films was carried out through alternately spraying the polyelectrolyte aqueous solutions on a perpendicularly fixed PDMS sheet with spray bottles "air-boy" (Carl Roth GmbH, Germany), just as described in refs 15 and 28. In our case, the PSS solution was sprayed two sequential times (5 s duration each) with 15 s waiting time after each time spraying, followed by 5 s water washing and subsequent 15 s waiting; then the PDDAC solution was sprayed by the same process followed by N_2 drying to obtain one PDDAC/PSS bilayer. $(PDDAC/PSS)_n$ multilayers with a designed bilayer number can be prepared after simply repeating the above spraying assembly cycles for *n* times.

Fabrication of Well-Defined Wrinkles of Multilayer Films by Embossing. The above surface-perfluorinated silicon master was stamped with a pressure of ~2 MPa on the multilayer films which were deposited on the elastomeric PDMS substrate. The stamping process was carried out when the multilayer films were kept in air (referred to as dry embossing) or immersed in water (referred to as wet embossing). After a given time of compression, the master was detached and the printed multilayer films were further immersed in water for a given time followed by nitrogen drying. The air humidity was about 30%.

Characterization. Atomic force microscope (AFM) images were obtained in tapping mode on a nanoscope IIIa Multimode scope (Digital Instruments Inc., Santa Barbara, CA) with silicon cantilevers (NC-W, the typical frequency of 285 kHz). Optical microscope images were recorded using an Axioskop 2 microscope equipped with a charge-coupled device (CCD) camera. The structured silicon wafer was characterized with scanning electron microscopy (SEM) on a Gemini LEO 1550 instrument operated at 3 kV.

Results and Discussion

Figure 1 shows the schematic illustration of the three-step procedure for creating well-defined wrinkles of multilayer films on a soft support. At first, a three-layer substrate consisting of a bulk PDMS support, a hard silica-like (SiO_x) layer, and a polyelectrolyte multilayer is produced. This is done by plasma treatment of the PDMS

(20) (a) Khang, D.-Y.; Jiang, H. Q.; Huang, Y.; Rogers, J. A. *Science* **2006**, *311*, 208. (b) Khang, D.-Y.; Xiao, J. L.; Kocabas, C.; MacLaren, S.; Banks, T.; Jiang, H.; Huang, Y.; Rogers, J. A. *Nano Lett.* **2008**, *8*, 124.
(21) Chan, E. P.; Smith, E. J.; Hayward, R. C.; Crosby, A. J. *Adv. Mater.* **2008**, *20*, 711.
(22) Ohzono, T.; Watanabe, H.; Vendamme, R.; Kamaga, C.; Kunitake, T.; Ishihara, T.; Shimomura, M. *Adv. Mater.* **2007**, *19*, 3229.
(23) Mertz, D.; Hemmerle, J.; Mutterer, J.; Ollivier, S.; Voegel, J. C.; Schaaf, P.; Lavalle, P. *Nano Lett.* **2007**, *7*, 657.
(24) Lim, J. H.; Lee, K. S.; Kim, J. C.; Lee, B. H. *Opt. Lett.* **2004**, *29*, 331.
(25) Smoukov, S. K.; Bitner, A.; Campbell, C. J.; Kandere-Grzybowska, K.; Grzybowski, B. A. *J. Am. Chem. Soc.* **2005**, *127*, 17803.
(26) Chung, J. Y.; Youngblood, J. P.; Stafford, C. M. *Soft Matter* **2007**, *3*, 1163.
(27) Kim, D.-H.; Shin, D.-S.; Lee, Y.-S. *J. Pept. Sci.* **2007**, *13*, 625.

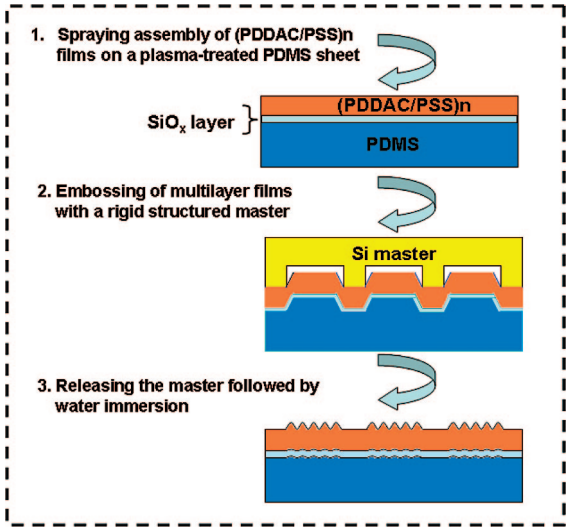

Figure 1. Schematic illustration of a three-step procedure for regioselectively creating well-defined wrinkles of multilayer films on an elastomeric PDMS substrate.

which creates a SiO_x surface layer and subsequent LbL coating. In the second step, the three-layer substrate is embossed in air (i.e., dry embossing) or in water (i.e., wet embossing) using a structured silicon wafer. In the final step, the substrate is annealed in water after releasing the silicon master.

In the particular case, the 2 min plasma-treated PDMS was utilized as the substrate to fabricate PDDAC/PSS multilayers in all of following experiments, except those specifically stated. Here $(PDDAC/PSS)_n$ films are fabricated by the LbL spraying assembly, which is highly efficient in the film buildup while maintaining the film quality and film interior nanostructure comparable to the typical dip immersion-based LbL assembly.[15,28] It is seen that the thickness increment of each PDDAC/PSS bilayer, determined by AFM, is around 3.4 nm. Additionally, structured silicon wafers with two types of typical recessed or protruding areas are utilized to emboss the underlying multilayers. One has isolated protruding areas (simply referred to as type A) with different morphologies such as square pillars, as shown in Figure 2a,b. So the compressed areas of the silicon master with the multilayers are also separated from each other. The other has isolated recessed areas (simply referred to as type B) while the compressed areas of the silicon master with the multilayers are continuous (Figure 2c,d).

At first, we investigate surfaces that result from a dry embossing process with the silicon master of type A. Figure 3a shows the AFM height image of the multilayer films embossed for 5 min. From the inset of the zoomed three-dimensional AFM image, it is clearly seen that the films have lotus-shaped morphologies with a peripheral size of 8−9 μm in diameter for every hollow "lotus" structure. Obviously it is bigger than and also different from the corresponding 5 μm-sized square pillar of the master (Figure 2a,b). When compared with the used master, one can notice that the middle hollow part lower than the surrounding wrinkles corresponds to the contact region of the films with the structured master. When exposed to water, the lotus-shaped wrinkles, which are stable in air, disappear immediately and evolve into a pattern of troughs surrounding each 5 μm-sized square contact area (Figure 3b). During the above morphological transformation we have not observed cracks and delamination of multilayers from the PDMS substrate. From its cross-section analysis (Supporting Information Figure S1), we deduce depth and width of the trough. For the $(PDDAC/PSS)_{40}$ multilayers, the resultant trough templated by the 5 μm-sized pillars is about 890 nm wide and 530 nm deep on average, respectively. Furthermore, both width and depth of the trough increase linearly with the thickness of the multilayer films (i.e., bilayer number n; Figure 3c,d). Considering the slopes in Figure 3 c,d, the increment in the width and the depth contributed by each PDDAC/PSS bilayer is estimated to be roughly 4.5 and 6.5 nm from the 5 μm-sized pillared master, roughly 8.7 and 6.7 nm from the 10 μm-sized pillared master, respectively. These results indicate that the morphology of the trough can be easily manipulated by the thickness of the assembled films and the size of the protruding pillars of the structured master. The existence of the intercept indicates an influence of the plasma-treated PDMS sheet on the resulting trough. On the other hand, when the embossing time in air is extended beyond 1 h, the embossed films have the above surface relief structures of circled troughs no matter whether the films have been exposed to water or not (data not shown here).

When the embossing was carried out in water, the as-stamped multilayer films exhibit a completely different surface contour morphology (Figure 4), as compared with those embossed in air (Figure 3). Before the water-immersion post-treatment, the $(PDDAC/PSS)_{40}$ printed films from the above 5 μm-sized pillared patterns of the master have novel concentric wrinkles with 1−2 μm wavelengths and 50−150 nm amplitudes. These wrinkles circle around each contact part until the outermost circled wrinkles are tangential to each other (Figure 4a). The zoomed AFM height image (inset of Figure 4a) further shows the concentric wrinkles, especially for those near to the printing area, having hierarchical structures with a bigger wavelength of wrinkles composed of several smaller wavelengths (i.e., 225 nm). After re-exposure to water, the wrinkles with a bigger wavelength seem not stable and the amplitude decreases drastically just as previously reported.[14a,15b,23] In contrast, the wrinkles of smaller wavelengths are stable and further developed outward at the expense of the original bigger ones (Figure 4b). However, it is still apparent that a new periodicity (600 nm) of wrinkles is formed, indicated by the marked Arabic number in the inset of Figure 4b and Figure S2a (Supporting Information). When the multilayers are stamped in water with 10 μm-sized pillared patterns of a master followed by water post-treatment, highly regular defect-free concentric wrinkles are produced with an average 275 nm wavelength and 20−50 nm amplitude (Figure 4c,d and Supporting Information Figure S2b). The periodicity of the wrinkles is similarly dependent on the size of the contact regions with a larger wavelength of wrinkles from

(28) (a) Schlenoff, J. B.; Dubas, S. T.; Farhat, T. R. *Langmuir* **2000**, *16*, 9968. (b) Izquierdo, A.; Ono, S. S.; Voegel, J.-C.; Schaaf, P.; Decher, G. *Langmuir* **2005**, *21*, 7558.

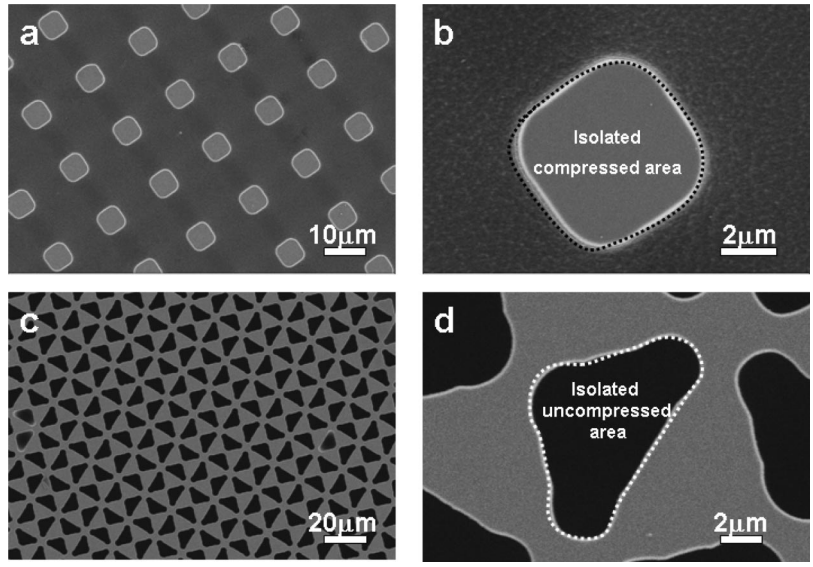

Figure 2. Typical SEM images of silicon masters with isolated protruding (type A) (a, b) and recessed (type B) (c, d) structures, respectively. The circled part in the corresponding zoomed SEM images represents the isolated compressed area (b) and the isolated uncompressed area (d) of the silicon master with the multilayers, respectively.

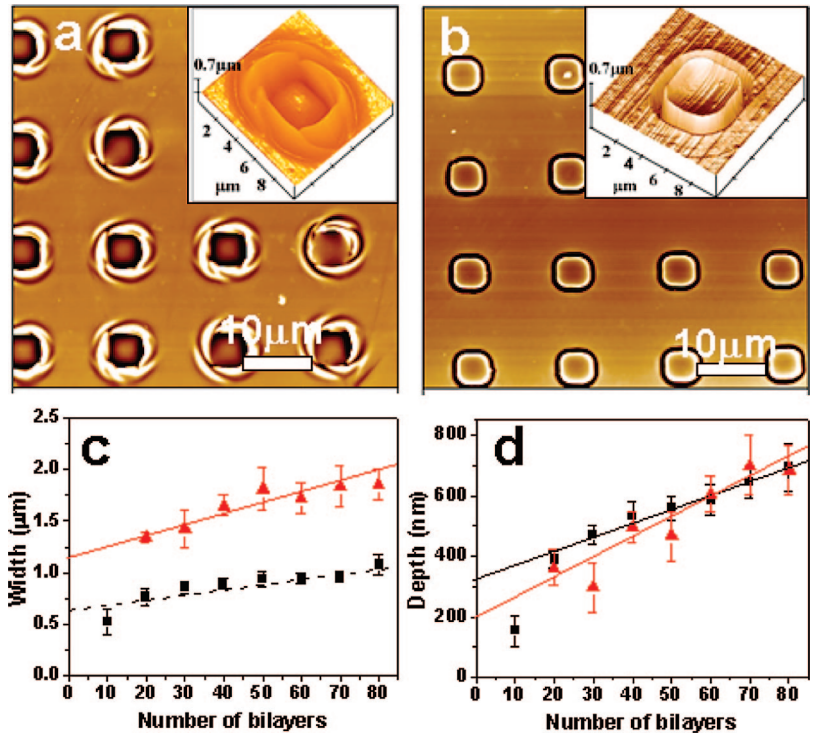

Figure 3. AFM height images of $(PDDAC/PSS)_{40}$ wrinkled multilayers embossed by 5 μm-sized pillared patterns of masters in air for 5 min (a), followed by 2 min water immersion (b); height scale: 700 nm. Parts (c) and (d) show the plots of the width and the depth of the resultant troughs on $(PDDAC/PSS)_n$ multilayers from 5 (■) and 10 μm (▲)-sized pillared patterns of the masters as a function of bilayer number (n), respectively.

a larger size of master patterns, just as those printed in air followed by water immersion. It is noted that the above concentric wrinkles of polyelectrolyte multilayers are very stable and can be subjected to water immersion for days.

Subsequently we varied the type of pattern to check the universality of structure formation. We utilized embossing forms with different sizes of protruding stripes to stamp the multilayer films in water. Just as expected, after releasing the master followed by water treatment, we obtained highly ordered stripes of wrinkles at a large scale. These stripes are free of defects that are always observed in the formed wrinkles.[5,6,15,22] Under the same conditions, the number of wrinkles can be simply controlled by the stripe sizes of the template (Figure 5). For instance, 7, 6, 4, 3, and 2 stripes of wrinkles are formed in the case of 4, 3.5, 2.5, 1.5, and 1 μm-sized stripes of patterns used, respectively.

So far, a master with isolated protruding pattern (Figure 2a,b) was used and the printed region on the multilayers was also separated, resulting in the formation of circled wrinkles around the contact area. We also employed a master with a concave pattern where compression was performed on a continuous phase and uncompressed areas were isolated

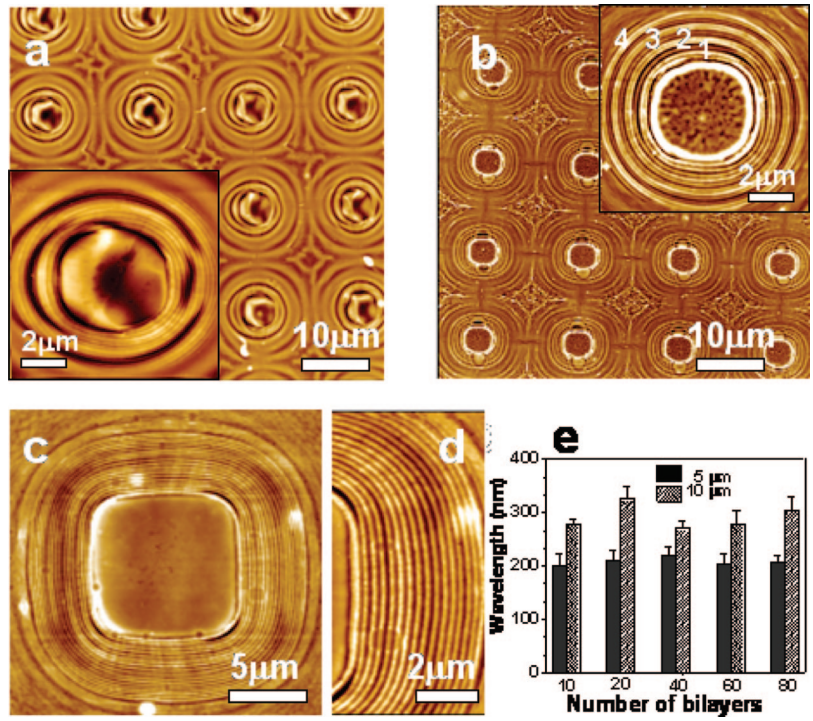

Figure 4. AFM height images of $(PDDAC/PSS)_{40}$ wrinkled multilayers embossed by 5 (a,b) and 10 (c,d) μm-sized pillar patterns of the masters in water for 1 h (a), followed by 2 min water immersion (b-d); height scales: 500 (a) and 150 (b−d) nm, respectively. Part (e) represents the effect of bilayer numbers (n) on the wavelength of the $(PDDAC/PSS)_n$ wrinkled films resulting from different sizes of pillar patterns, respectively.

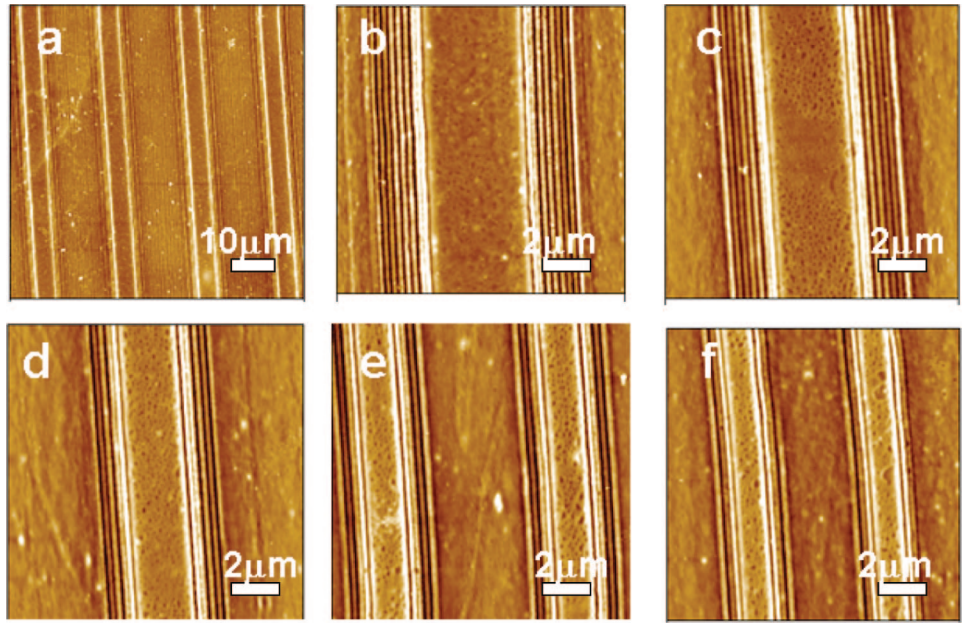

Figure 5. AFM images of as-prepared $(PDDAC/PSS)_{40}$ multilayer films stamped by a master with different sizes of stripes of patterns in water for 1 h followed by 2 min water immersion. Height scale: 100 nm.

(Figure 2c,d). Consequently, the induced wrinkles are well-confined in the isolated noncontact area, just as shown in Figure 6. Similarly, more regular concentric wrinkles are formed near the contact area while less ordered ones are generated far from the contact area. Explanation of the more complex pattern observed near the center is at this stage not possible.

To better understand the reason for the development of this fine-structure, we varied the parameters of the wet embossing process systematically. We found that the stamping time has no marked effect on the wavelength (Figure 7) and on the amplitude (not shown here) of the wrinkled films. This suggests that diffusion and movement of the wet-state multilayer film from the contact region to the contact-free one plays a negligible role in the above structure formation. This result is in contrast to findings of Shen et al. who embossed on multilayers on a rigid support,[29] indicating a dominant role of the soft support in our case. In earlier work

(29) Lu, Y.; Chen, X.; Hu, W.; Lu, N.; Sun, J. Q.; Shen, J. C. *Langmuir* **2007**, *23*, 3254.

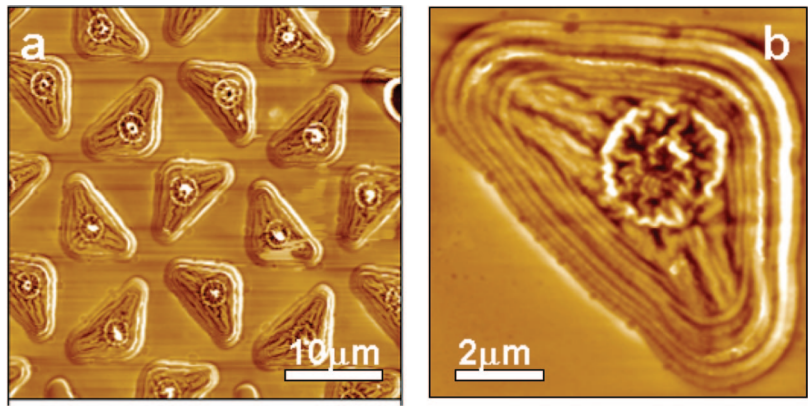

Figure 6. AFM height images of as-prepared $(PDDAC/PSS)_{40}$ multilayers embossed by the type B master in water for 1 h followed by 2 min water immersion. Height scale: 300 nm.

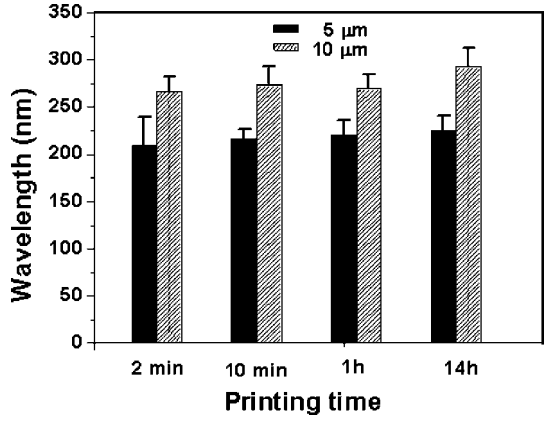

Figure 7. Effect of embossing time on the wavelength of the resultant $(PDDAC/PSS)_{40}$ wrinkled films prepared from different sizes of pillar patterns in water followed by 2 min water treatment, respectively.

on wrinkle formation of polymeric layers on an elastomeric support,[8,14,15a] a linear relationship between wrinkle wavelength and layer thickness has been found and explained using continuum mechanical theories.[8] Here we have systematically varied the layer thickness in our case and find that the wavelength of the induced wrinkles is independent of the thickness of the assembled polymeric multilayers (Figure 4e).

As the thickness of the multilayer had no influence on the periodicity of the wrinkles produced from wet embossing, we investigated the influence of the silica-like (SiO_x) layer thickness on this parameter. The thickness of this layer is determined by the time of the plasma treatment, and we consequently varied this parameter. We performed a control experiment in which PDMS substrates were plasma treated but not coated by multilayers prior to embossing. For 2 min of plasma treatment, concentric wrinkles with average wavelength of 250 ± 50 nm and amplitude below 4 nm are generated around the contact area (Figure 8). Thus the periodicity of the patterns is comparable to the case of embossed multilayers, while the amplitude is at least 1 order of magnitude lower. When the plasma treatment time of the PDMS was increased to 20 min, wrinkles with a bigger wavelength of 1 ± 0.25 μm were found (Figure 9a−c). Therefore, the wavelength of the embossed multilayers seems to be rather determined by the thickness of the SiO_x layer.

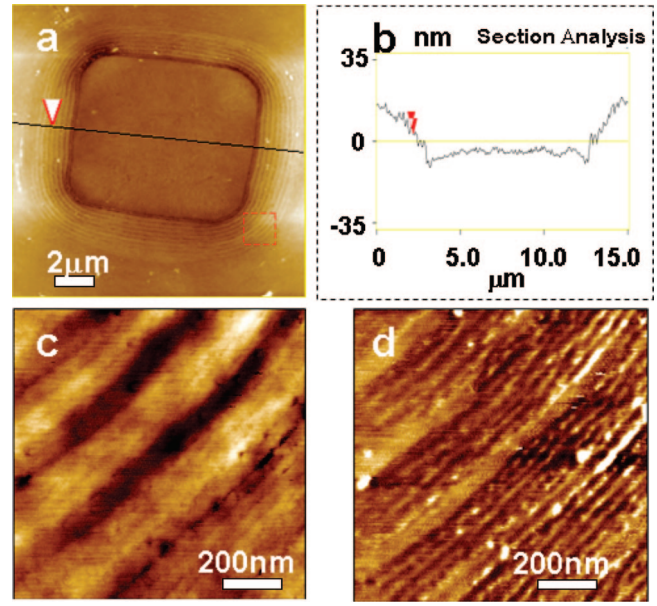

Figure 8. AFM height (a,c) and phase (d) images of a 2 min plasma-treated PDMS sheet stamped in water for 1 h followed by water immersion. The circled part of the image (a) is zoomed and shown in the images of (c) and (d). Plot (b) is the AFM cross section analysis of (a). Height scales: 75 (a) and 10 (c) nm, respectively; phase scale: 10°(d).

Indeed, when substrates were plasma treated for 20 min and subsequently multilayer-coated and embossed, the wrinkle periodicity shifted to a much larger periodicity (Figure 9d−f), compared with the result of 2 min plasma treatment shown in Figure 4. Still, the amplitude (∼100 nm) of the wrinkles formed by embossing the multilayer structures was larger than for the "blank" plasma treated substrates (20−30 nm, Figure 9c,f), and also larger than that of 2 min plasma treatment shown in Figure 4 and Figure S2 (Supporting Information).

On the basis of the above results, we conclude that when the hard master is embossed into the ultrathin multilayers that have been deposited on the thick PDMS elastomeric substrate, the contact-free regions of the multilayers, especially around the contact region, are subjected to stretch accompanied by deformation of the underlying softer support. The stretch direction is perpendicular to the contact borderline of the multilayers with the master, and the formed strain will be attenuated monotonously into the direction away from the contact region. When the load is released and the master

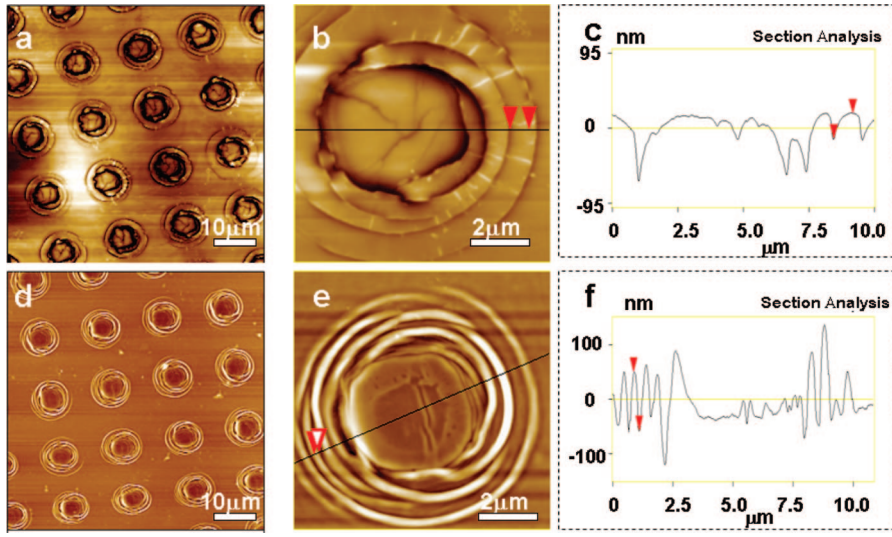

Figure 9. AFM images of a 20 min plasma-treated PDMS sheet (a, b) and its surface-coated $(PDDAC/PSS)_{40}$ films (d, e) both stamped in water for 1 h followed by water immersion. Plots (c) and (f) are the AFM cross-section analysis of (b) and (e), respectively. Height scales: 100 (a, b) and 300 (d, e) nm, respectively.

is detached from the multilayers, the compressed part of the PDMS elastomeric substrate resumes the original strain-free state quickly, while the hard multilayer shows partially inelastic deformation. As a result, compressive stress is produced at the PDMS support/multilayer interface and selectively distributed around the contact area. The direction of the formed stress is perpendicular to the contact borderline of the multilayers with the master. To obtain a minimum system energy in the case of the relaxation of the compressive stress,[2−13] well-confined surface relief structures are generated in the form of concentric wrinkles around the contact area, and their direction is perpendicular to the compressive stress and parallel to the contact borderline. Of course, the produced compressive stress is related to not only the interior structures of the support/multilayer system but also to the external load and to the geometry of the printing master. Under the same conditions, the bigger the size of the printing master, the smaller the stress. Therefore we observe the dependence of the wrinkles on the size of the master.

The wavelength of the wrinkles is determined by the thickness of the hard silica-like (SiO_x) top layer and thus dependent on the plasma treatment duration. Indeed, the observed wavelengths can be well explained using the established analytical relation for the wrinkle wavelength (eq 1),[8]

$$E_f = \frac{3E_s(1 - V_f^2)}{1 - V_s^2}\left(\frac{\lambda}{2\pi d_f}\right)^3 \qquad (1)$$

where d is the thickness of the SiO_x layer, V is Poisson's ratio, λ is the wrinkling wavelength, and E is the Young's modulus (subscripts f and s represent the formed silica-like layer film and the PDMS substrate, respectively). Under our experiment conditions, the wavelengths (λ) of the 2 and 20 min plasma-treated PDMS substrates of 250 ± 50 nm (Figure 8) and 1 ± 0.25 μm (Figure 9a−c), respectively, correspond well to the thickness d_f = 1.8 ± 0.3 nm (for 2 min plasma treatment) and 7.2 ± 1.8 nm (for 20 min plasma treatment) of the silica-like layer according to eq 1 in the case of E_f = 70 GPa, E_s = 1.8 MPa, V_f = 0.33, and V_s = 0.5.[18] It is pointed out that the silica-like surface layer of the PDMS is composed of a dense silicate layer and an intermediate diffuse silicate layer with a varying silica density with plasma treatment.[30] Here it is just simplified as one dense SiO_2 layer, and the estimated thickness is also close to the reference value of 5 nm.[31] We are aware of the fact that eq 1 considers elastic deformations. Our reasoning, however, is that these are followed by cracks as inelastic processes. A possible explanation for the fact that the periodicity of the silica film's wrinkles determines the periodicity of the multilayers after annealing would be a partial chemical modification of the silica due to the wrinkling, partially similar to the spatial forcing effect of the preformed underlying trigger patterns on the subsequent surface wrinkling.[22] It is well-known that silica is rather inelastic and easily cracks under strain. Indeed, cracks along the wrinkles are visible in Figure 9a,b. In case the silica layer cracks, the hydrophobic PDMS is exposed to the multilayer, which is unfavorable from a wetting point of view. Therefore, we suggest that the multilayer is dewetting from the cracked regions in the annealing step. Thus the periodicity of the structures is determined by the crack periodicity, while the amplitude is determined by the multilayers. This mechanism explains as well the increased aspect ratio of the wrinkle patterns, compared with the control plasma-treated PDMS. This is further supported by the fact that on reducing the applied force from 2 to 1 MPa the amplitude of the resultant wrinkles decreases but the wavelength remains almost the same. Obviously the observation opens further perspectives for structuring: Usually it is difficult to achieve a reasonably high aspect ratio by wrinkling, since the periodicity and the aspect ratio of the wrinkles are coupled to each other. In this case, we decouple both quantities by using a two-layer film, in which one layer determines the wavelength of the pattern (by introducing a wetting contrast) and the second layer determines the amplitude.

(30) Hillborg, H.; Tomczak, N.; Olah, A.; Schonherr, H.; Vancso, G. J. *Langmuir* **2004**, *20*, 785.
(31) Efimenko, K.; Wallace, W. E.; Genzer, J. *J. Colloid Interface Sci.* **2002**, *254*, 306.

Conclusion

In summary, embossing of polyelectrolyte-multilayer coated, plasma treated surfaces can be used to construct well-defined surface relief structures of highly ordered concentric wrinkles with remarkably small wavelength (down to 250 nm). We found that the observed wrinkle periodicity does, within experimental accuracy, not depend on the multilayer thickness, but is rather determined by the properties of the thin SiO_x layer formed in the plasma treatment step. In contrast, the amplitude of the patterns scaled with the multilayers. We explain this observation by combined effects of wrinkling and dewetting and suggest that a wetting contrast is introduced in the wrinkling process by periodic cracks of the SiO_x layer, and the final structure is formed by adaptation of the multilayer to this hydrophobic pattern. We believe that this new mechanism of pattern formation via an inelastic deformation combined with wettability contrast cannot only pave the way toward overcoming the limitations in achieving high aspect ratio of structures using the wrinkling approach but also allow producing hierarchically structured patterns consisting of micrometer-scale patterning given by the embossing stamp and the submicrometer scale structure due to the wrinkles which were previously not accessible. Furthermore, the improved stability over many days of the wrinkles of polyelectrolyte-based multilayers greatly extends their potential application to wet surroundings such as in controlling wettability[26] and as structured templates directing aligned particles[15b] and for further patterning.[25] Of course, more experiments and theoretical models need to be designed to support and validate the new mechanism of wrinkling in the future.

Acknowledgment. The work was financially supported by the Max Planck Society by a research fellowship. C.L. also thanks Anneliese Heilig and Dr. Zhenwei Mao for their help in the AFM measurement and SEM characterization, respectively.

Supporting Information Available: Detailed AFM cross-section analysis of the as-prepared trough and concentric wrinkles (PDF). This information is available free of charge via the Internet at http://pubs.acs.org.

CM8018742